RSC Advances

PAPER

Cite this: *RSC Adv.*, 2024, **14**, 6199

Switchable surface and loading/release of target molecules in hierarchically porous PLA nonwovens based on shape memory effect†

Lishuo Zhang,[ab] Wenqiang Chai,[c] Jiaru Zhang,[b] Zhouli Chen,*[d] Ziyang Yue,*[e] Jiayao Wang *[b] and Jiankang Yu[a]

Received 9th December 2023
Accepted 9th February 2024

DOI: 10.1039/d3ra08411f

rsc.li/rsc-advances

In this work, hierarchically porous PLA (polylactic acid) shape memory nonwovens were prepared by electrospinning its blend solution with PEO (polyethylene oxide) and subsequent water etching. Based on shape memory effect resulting from tiny crystals and the amorphous matrix of PLA, the switch between compact and porous surfaces has been achieved *via* cyclical hot-pressing and recovery in a hot water bath. After hot-pressing, the disappearance of hierarchical pores contributes to compact surface, enabling embedding of the target molecule in PLA nonwoven (*i.e.*, CLOSE state). Upon exposure to heat, PLA nonwoven recovers to its permanent shape and exhibits a porous surface, providing a penetrative diffusion pathway for small molecules (*i.e.*, OPEN state). The hierarchically porous structure and shape memory effect endow PLA nonwoven with the capability of rapid release. Our results provide a good candidate for some potential applications, such as temperature-controlled quick-release of catalysts and drugs.

1. Introduction

Porous materials have been widely used in different kinds of applications, in which porosity, pore size and geometry are key factors.[1–3] The manipulations of them were achieved mainly *via* parameter optimization during preparation.[4] In the past decades, the concept of stimuli-responsive porous materials (SRPMs) has been reported.[5,6,8–10] Relative to traditional ones, the porous structures in SRPMs can be tailored after the preparation of them. The developed post-treatment strategy brings more possibilities for the precise manipulation of pore size/geometry and porosity, which is significant for the controllable release of the drug.[7,11,15] So far, two kinds of strategies have been developed to fabricate SRPMs. On the one hand, they were prepared by incorporating stimuli-responsive materials on the pore wall. For instance, Chu introduced stimuli-responsive (thermo-, pH-, ion-, molecule- and UV-light-responsive) molecules to porous membranes using "grafting-from" and "grafting-to" methods.[11] On the other hand, the porous structures in the microscale can be tailored *via* deformation in the macroscale. For instance, Zhu *et al.* synthesized a stretchable porous nanocomposite *via* a sacrificial template method in which carbon nanotubes (CNTs), prepolymer of poly dimethylsiloxane (PDMS) and sodium chloride (NaCl) were mixed, followed by curing of PDMS and the removal of NaCl *via* water etching. The resultant nanocomposites exhibit sponge-like porous structures which can be manipulated with the help of cyclical deformation (compressing) and recovery (unloading).[12]

Shape memory polymers (SMPs) are smart materials that can be fixed as temporary shape and recover the permanent shape upon external stimulus.[13,14] There have been some reports focusing on drug release based on shape memory effect.[15–17] In most of them, drugs were loaded by means of swelling or mixing in polymer matrix. It always takes long period for the drug molecule to diffuse through the tortuous pathway, contributing to slow release.[18–21] For instance, Liu *et al.* prepared long-term drug release membranes by electrospinning. The results show that the swelling and degradation of poly(D,L-lactide-*co*-glycolide) (PLGA) fibers determined the release rate of drugs.[22] Lian *et al.* employed melt electrospinning for the development of daunorubicin hydrochloride-loaded poly(ε-caprolactone) (PCL) fibrous scaffolds. The high crystallinity of the nonwoven resulted in slow-release rates and long-term release periods for more than 16 days.[23] In some cases, however, higher release speed is desired, *e.g.*, rapid drug release in gastrointestinal tract triggered by environmental variations.[24–26] In our previous work, shape memory effect has been introduced to porous materials.[27]

[a]*College of Safety Science and Engineering, Liaoning Technical University, Huludao, 125105, China*

[b]*College of Material, Chemistry and Chemical Engineering, Hangzhou Normal University, Hangzhou, 311121, China. E-mail: Jiayao-wang@outlook.com*

[c]*Tongxiang Jianmin Filter Material Product Co. LTD., 314511, Jiaxing, China*

[d]*Zhejiang Institute of Mechanical & Electrical Engineering, Hangzhou, 311203, China. E-mail: xiaoliu1018@126.com*

[e]*College of Science, Liaoning Technical University, Fuxin, 123000, China. E-mail: 13591995463@163.com*

† Electronic supplementary information (ESI) available. See DOI: https://doi.org/10.1039/d3ra08411f

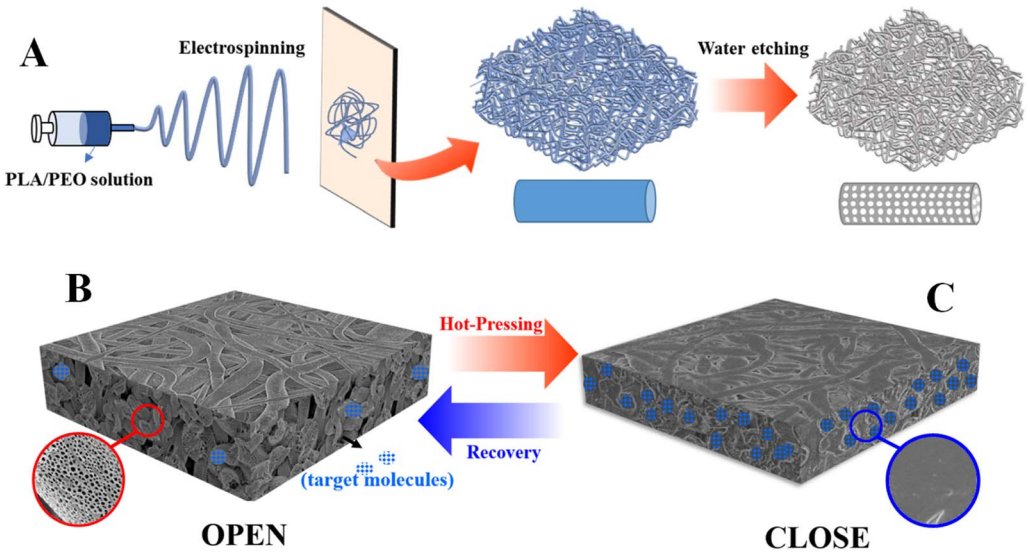

Scheme 1 Cartoon illustration of loading (B) and release (A) of target molecules in PLA porous shape memory nonwovens.

Relative to traditional stimuli-responsive materials, porous shape memory polymers are excellent candidate for rapid release of drugs since they exhibit exciting features. For one thing, they can be used without loading (compared with elastomer, *e.g.*, PDMS), corresponding to a low-energy-consumption situation.[28] For another thing, the permeation pathway of target molecules in them can be tailored precisely.[29] However, it is still a great challenge to load target molecules into porous materials based on shape memory effect so far because of the absence of complete "CLOSE" state.

In this work, polylactic acid (PLA) nonwovens with both shape memory effect and hierarchical pores have been fabricated by electrospinning its blend solution with PEO (polyethylene oxide) and subsequent water etching (to remove PEO) (Scheme 1A) since electrospinning has been employed to prepare nonwoven (including shape memory polymers) successfully in the past decades.[30–32] It is proposed to load and release target molecules as follow. For one thing, it is facile to obtain compact surface *via* hot-pressing and fix it as a temporary shape based on shape memory effect. This is an efficient way to load target molecules in porous nonwoven (Scheme 1C). For another thing, PLA shape memory nonwovens can recover to the permanent shape spontaneously upon the exposure to heat (Scheme 1B), producing porous surface. The resultant penetrative diffusion pathway endows our specimen with the ability to release the loaded target molecules (Scheme 1B).

2. Experimental section

2.1. Materials and sample preparation

PEO ($M_w = 100\,000$ g mol^{-1}) and PLA ($M_n = 89\,300$ g mol^{-1}, PDI = 1.77) were purchased from Alfa Aesar and Nature Works respectively. PLA nonwoven was obtained *via* electrospinning PLA/PEO (weight ratio 1/2) blend solutions (10 wt% in chloroform). The applied electrospinning voltage, flow rate and tip-to-collector distance were 15 kV, 0.2 mL h^{-1} and 15 cm, respectively.[33] After electrospinning, the nonwoven was immersed in water (24 hours) to remove PEO, followed by being kept in vacuum (6 hours). The complete removal of PEO can be confirmed by DSC and TGA shown in the ESI (Fig. S1†).

2.2. Sample characterization

The morphologies of PLA nonwoven (surface and cross-section) were measured with the help of Scanning Electron Microscope (Japan, Hitachi S-4800) with an operating voltage of 3 kV and a distance of 8 cm. To load Coomassie blue (G-250) into PLA porous nonwoven, the specimen was kept in G-250 solution (3 wt%) for 1 hour, followed by drying in vacuum for 2 hours (the drying step is important to improve the loading efficiency). Then, the porous shape memory nonwoven (with G-250) was hot-pressed at 65 °C for 2 minutes (30 MPa) and cooled to room temperature with the help of cycling water (~2 min). To release G-250, the hot-pressed specimen was put in water bath preheated to various temperatures. The UV-vis transmittance of released CB was collected in the 400–800 nm wavelength region using a spectrophotometer (UH5300, Hitachi, Japan).

3. Results and discussion

Fig. 1 shows the SEM images of as-prepared specimen. In Fig. 1A, there are porous fibers in various directions whose diameters locate at several microns (the original average diameter of PLA fibers is 3.8 μm and the distribution can be found in Fig. 2I). To observe the morphologies of PLA porous nonwoven in membrane thickness direction, SEM image of cross-section was taken. In Fig. 1B, there is obvious space among neighboring fibers. In other words, these fibers pack in loose manner, contributing to pores in microns. Then, our attention has been paid to the surface morphology of PLA fiber. In SEM image with higher magnification (Fig. 1C), we can find some pores whose diameter ranges from hundreds of

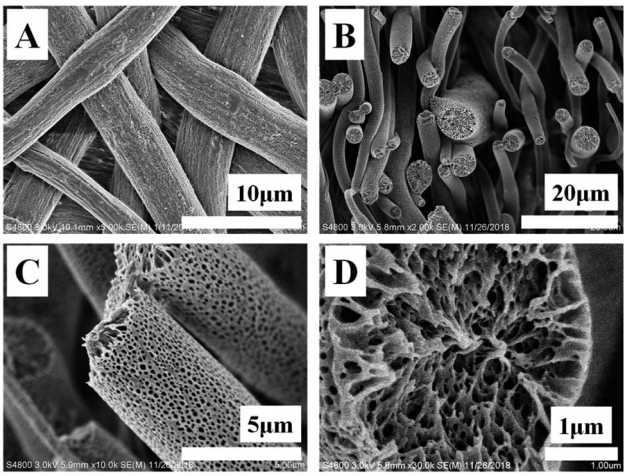

Fig. 1 SEM images of surface (A), cross-section (B) and certain fiber (C and D) of PLA porous shape memory nonwoven.

nanometers to several microns. The formation of them can be interrupted briefly as follow.[34] During electrospinning PLA/PEO blend solution, phase segregation between them occurs since PEO crystallizes very quickly, producing bi-continuous structures of PLA and PEO. Porous PLA can be obtained upon water etching due to the solubility of PEO in water. As a result of this kind of bi-continuous structure from crystallization template, there are penetrative pores through the whole fiber (Fig. 1D). The DSC and TGA can be employed to confirm the complete removal of PEO. As shown in Fig. S1A,† before water etching, the melting peaks located at 59.5 °C and 166.6 °C correspond to the melting behavior of PEO and PLA crystals, respectively. After etching, the melting peak at 59.5 °C disappeared, corresponding to the complete removal of PEO. In the results shown in Fig. S1B,† the fibers of PLA/PEO blend exhibit two weight losses. It is obvious that the composition of PLA and PEO is 33.9% and 66.1% respectively, which has a good agreement with the composition in PLA/PEO solution before electrospinning. After water etching, there is only one weight loss corresponding to the thermal degradation of PLA. According to the discussion above, it is clear that there are hierarchically porous structures in PLA nonwovens including pores in microns (among neighboring fibers) and pores in nanometers (on fibers). These pores provide sufficient space to load target molecules in nonwovens.

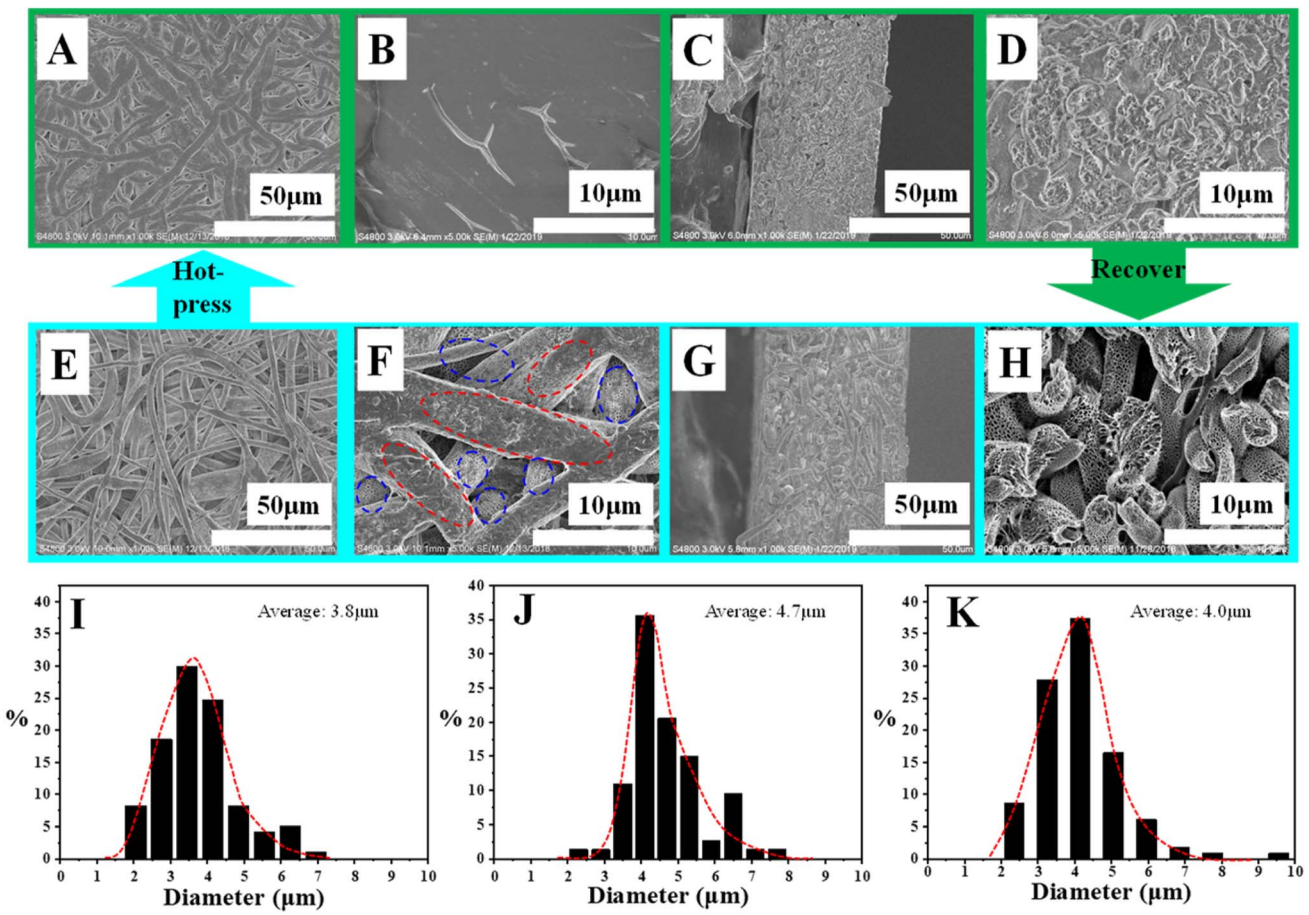

Fig. 2 SEM images of hot-pressed (A to D) and recovered (E to H) specimens. Images of (A), (B), (E) and (F) show the surface of PLA nonwoven with lower (A and E) and higher (B and F) magnification. Images of (C), (D), (G) and (H) demonstrate cross-section of specimen with lower (C and G) and higher (D and H) magnification; the average diameter of the fibers before hot-pressing (I), after hot-pressing (J) and after recovered in hot water bath (K).

PLA is a typical semi-crystalline polymer with very low crystallization rate, producing tiny crystals and amorphous matrix upon cooling to room temperature from melting state. According to the DSC data shown in Fig. S2,† the crystallinity of PLA can be calculated (~4.3%). The tiny crystals and amorphous matrix can play the role of shape-fixing phase and shape-recovery phase respectively. Therefore, PLA is an excellent thermoplastic shape memory polymer in which the glass transition temperature of it (at ~56 °C as shown in Fig. S2†) acts as switching temperature. As shown in Fig. S3A,† the as-prepared specimen is the permanent shape. When it was put in hot water bath (65 °C), it can be deformed to the desired shape which can be fixed by cooling down to room temperature with loading. This is so-called temporary shape (Fig. S3B†). Upon the exposure to heat, PLA nonwoven can recover to its permanent shape spontaneously (Fig. S3C†). Based on shape memory effect of PLA porous nonwoven, we can fabricate switchable surface *via* the combination of hot-pressing and recovery as follow. Hot-pressing at 65 °C (30 MPa) for 2 minutes yields compact surface (Fig. 2A). On one hand, the porous structures in each fiber have been destroyed since the operation temperature is above the glass transition temperature of PLA (Fig. 2B); on the other hand, the space among neighboring fibers disappears (Fig. 2A and B). In this case, it is impossible for small molecules to diffuse out of PLA nonwoven because of the absence of penetrative pathway. This is so-called CLOSE state. The resultant specimen exhibits higher density (0.29×10^{-3} kg m^{-3}, based on weight and volume) and mercury injection apparatus fails to measure its porosity due to the compact surface. The average diameter of PLA fibers increased to 4.7 μm due to shape changes under applied pressure (shown in Fig. 2J). When the hot-pressed specimen was immersed in water bath at high temperature (65 °C), PLA chain segments in amorphous matrix exhibit certain mobility, enabling the recovery to permanent shape. As a result, the morphology evolution occurs on the surface of PLA nonwoven. In Fig. 2E, the recovery results in some space among fibers. In Fig. 2F, the porous structures on the top part of surface (red dash ellipse) have not recovered to their original state completely (Fig. 1C). Other fibers (*e.g.*, in sublayer, blue dash ellipse), however, exhibit typical porous structures resulting from crystallization template.[18] In other words, parts of fibers recover to porous state upon the exposure to heat. The details can be found in Fig. S4.† After recovery, the density of PLA nonwoven decreases down to 0.23×10^{-3} kg m^{-3}. The porosity locates at ~80%. The average diameter of PLA fibers exhibited a recovery to 4.1 μm due to the shape memory effect of PLA (shown in Fig. 2K). The combination of space among fibers and porous structures in fibers contributes to penetrative diffusion pathway for small molecules, corresponding to OPEN state. During the switch between OPEN/CLOSE states discussed above, the structure evolutions in cross-section direction are shown in Fig. 2. Upon hot-pressing (Fig. 2C and D), the fibers pack so closely that there is no free space among them. The resultant nonwoven exhibits lower magnitude of thickness (~50 μm). Consequently, the disappearance of free space in thickness direction aggravates the CLOSE state. After the recovery in hot water bath, the nonwoven thickness increases to ~60 μm (Fig. 2G). As a result, there is obvious free space among neighboring fibers (Fig. 2H), enhancing the OPEN state. The switch between compact/porous surfaces (as well as lower/higher thicknesses) can also be realized in other operation conditions (Fig. S5 and S6†).

In the loading and release experiment, Coomassie blue (CB) has been employed as the model (target) molecule to show the main concept of loading and release due to the following points. (1) It is very facile to track it even by eyes; (2) it exhibits excellent thermal stability. As shown in Fig. 3A, the as-prepared PLA nonwoven was immersed in CB solution for 1 hour. After dried in vacuum for 2 hours, the nonwoven with CB molecules was hot-pressed at 65 °C for 2 minutes (30 MPa). This is an efficient

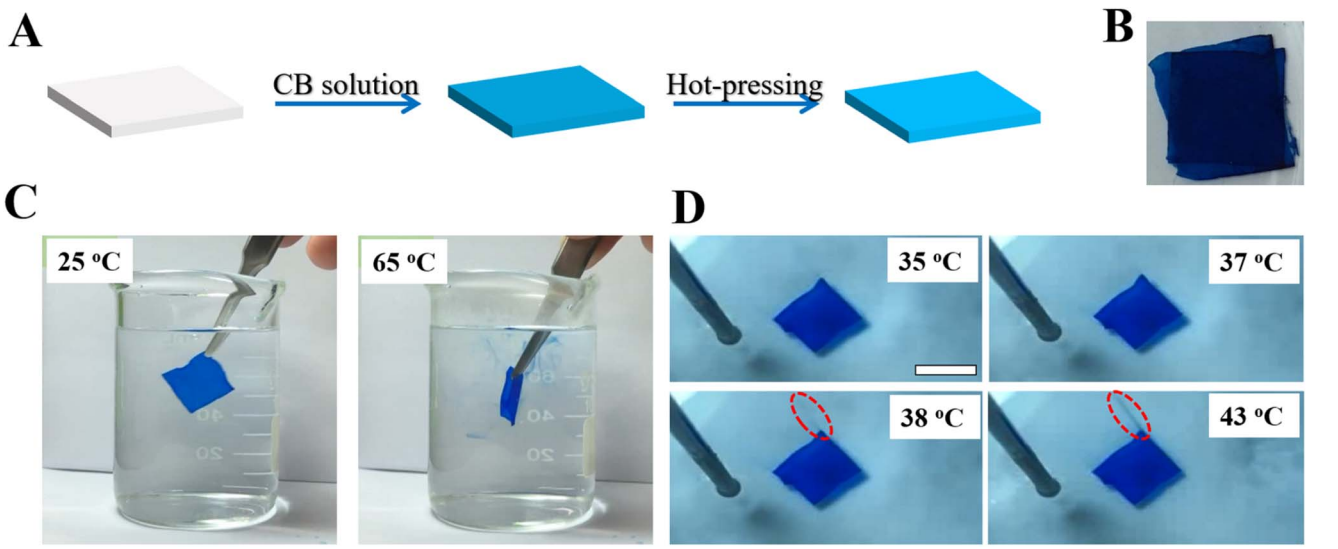

Fig. 3 Schematic illustration of loading of target molecules (A) and the photograph of resultant specimen (B). (C) shows the release of target molecules at the indicated temperatures while (D) demonstrates the release during continuous-heating process.

way to load target molecules into our porous specimen and prevent the diffusion of them into water since the nonwoven exhibits compact surface as shown in Fig. 2B. Fig. 3B is the photograph of PLA shape memory nonwoven with loaded CB. According to the results shown in Fig. 4, the loaded CB in hierarchically porous PLA nonwoven is 0.022 mg mg^{-1}. To simulate the release of target molecule, our specimen was put into water bath in two ways, *i.e.*, static release at certain temperature (Fig. 3C) and dynamic release during continuous-heating (Fig. 3D).[11,12] In the former, the release temperature was set at 65 °C and 25 °C (reference). In order to quantify the amount of released CB in water, a UV-vis spectrophotometer has applied to detect the releasing process of CB at different temperature. As shown in Fig. 3C and 4B, in reference (CLOSE state specimen set at 25 °C), there is no CB diffusing into water even for 1 hour. As for the OPEN state specimen which is set at 25 °C, CB dyes released very fast (shown in Fig. S9†), the finally actual amount of released CB in water is 0.007 mg mL^{-1} (shown in Fig. 4D). On the contrary, when our specimen was immersed in hot water bath (65 °C, right in Fig. 3C), we can find the CB dyes locally around the nonwoven immediately. At the same time, the specimen becomes flexible and changes its shape arbitrarily (Fig. S8†). Due to the destroyed porous structures on the top part of surface, the actual amount of released CB in water was 0.006 mg mL^{-1}, which is a little smaller than that in OPEN state specimen set at 25 °C. The static release result has good agreement with the structure evolution during hot-pressing and recovery (Fig. 2). In reference, there is no penetrative pathway for CB molecules to diffuse from PLA nonwoven to water (upper part in Fig. 2), corresponding to CLOSE state. In the case of 65 °C, the recovered porous structures in fibers and free space among fibers provide continuous diffusion pathway, accounting for OPEN state. In the specimen without hot-pressing, there are always releases of CB at both 25 °C and 65 °C (Fig. S9†). Obviously, the release of target molecule is no doubt a consequence of the penetrative diffusion pathway resulting from porous surface upon recovery (Fig. 2F). In bulky PLA, the switching temperature locates at 56 °C (Fig. S2†), the glass transition temperature of it. In PLA nonwoven with hierarchical pores, the sufficient contact between PLA and hot water can accelerate the shape recovery and reduce the switching temperature. To identify the exact switching temperature, a continuous heating experiment has been performed. As shown in Fig. 3D, PLA nonwoven with CB molecules was immersed in water bath at room temperature. Then, the bath was heated from 24 °C to 65 °C at the heating rate of 10 °C min^{-1}. At 35 °C and 37 °C, there is no CB dye in water. Upon further heating, we can find some dyes around the top corner (red dash ellipse) at 38 °C. The release of target molecules has been further enhanced when the temperature reaches 43 °C (red dash ellipse).

Then, we can describe the loading and release of target molecules in PLA porous shape memory nonwovens as follow (Scheme 1B and C). When PLA nonwoven with target molecules was hot-pressed at high temperature (above the switching temperature), the compact surface (Scheme 1C and Fig. 2A) prevents the diffusion of target molecules from it, contributing to the CLOSE state. Upon the exposure to heat, PLA fibers

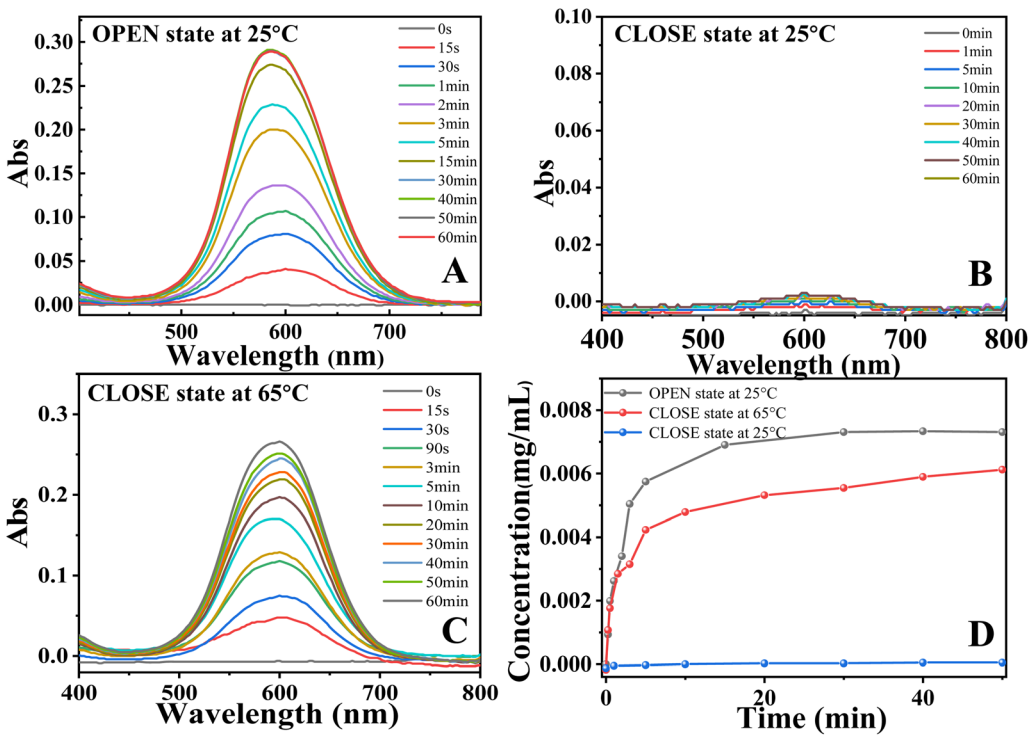

Fig. 4 UV-vis spectra for the CB solution during release process at different temperature (A–C) and the concentration of CB in water during release process (D).

recover to its permanent shape, producing pores in them and free space among them (Scheme 1B and Fig. 2E). This is the reason for the continuous diffusion pathway for target molecules and dyes in water (Fig. 3C and D), corresponding to OPEN state.

4. Conclusion

Hierarchically porous PLA nonwoven has been fabricated by electrospinning its blend solution with PEO and subsequent water etching. In resultant nonwoven, tiny crystal and amorphous matrix of PLA act as shape-fixing phase and shape-recovery phase respectively, contributing to shape memory effect. After hot-pressing, hierarchical pores disappear, leading to compact surface and enabling to load target molecules in PLA nonwoven (*i.e.*, CLOSE state). Upon the exposure to heat, the specimen recovers to its permanent shape and exhibits porous structures on fiber surface and among neighboring fibers. This is the reason for penetrative diffusion pathway and OPEN state. With the help of cyclical hot-pressing and recovery, it is facile to switch between two states discussed above, endowing the specimen with the ability to load and quick-release target molecules on demand. Our results provide a good candidate for some potential applications, such as precise synthesis (*e.g.*, catalyst loading), temperature-controlled quick-release of catalysis and drugs.

Conflicts of interest

There are no conflicts to declare.

Acknowledgements

This work was financially supported by National Natural Science Foundation of China (51973048).

References

1 A. D. Yancey, S. J. Terian, B. J. Shaw, T. M. Bish, D. R. Corbin and M. B. Shiflett, *Microporous Mesoporous Mater.*, 2022, **331**, 111654.
2 T. M. S. U. Gunathilake, Y. C. Ching, K. Y. Ching, C. H. Chuah and L. C. Abdullah, *Polymers*, 2017, **9**, 160.
3 Z. J. Wang, K. Q. Sun, Y. F. He, P. F. Song and D. W. Zhang, *Sci. Technol.*, 2019, **80**, 1266–1275.
4 I. Tokarev, V. Gopishetty and S. Minko, *ACS Appl. Mater. Interfaces*, 2015, **7**, 12463–12469.
5 L. J. Zhu, H. M. Song, C. Li, G. Z. X. Wang, Q. J. Zeng and J. Xue, *J. Membr. Sci.*, 2018, **555**, 290–298.
6 D. G. He, S. Wang, L. Lei, Z. T. Hou, P. Shang, X. X. He and H. M. Nie, *Chem. Eng. Sci.*, 2015, **125**, 108–120.
7 H. Y. He, E. Luedke, X. L. Zhang, B. Yu, A. Schmitt, B. McClarren, V. Grignol, W. E. Carson and L. J. Lee, *J. Controlled Release*, 2013, **165**, 226–233.
8 P. F. Li, R. Xie, H. Fan, X. J. Ju, Y. C. Chen, T. Meng and L. Y. Chu, *Ind. Eng. Chem. Res.*, 2012, **51**, 9554–9563.
9 J. Wei, X. J. Ju, X. Y. Zou, R. Xie, W. Wang, Y. M. Liu and L. Y. Chu, *Adv. Funct. Mater.*, 2014, **24**, 3312–3323.
10 B. A. Jana, U. Shinde and A. Wadhwani, *J. Biotechnol.*, 2020, **324**, 1–6.
11 Z. Liu, W. Wang, R. Xie, X. J. Ju and L. Y. Chu, *Chem. Soc. Rev.*, 2016, **45**, 460–475.
12 Y. J. Fan, X. S. Meng, H. Y. Li, S. Y. Kuang, L. Zhang, Y. Wu, Z. L. Wang and G. Zhu, *Adv. Mater.*, 2017, **29**, 1603115.
13 C. Liu, H. Qin and P. T. Mather, *J. Mater. Chem.*, 2007, **17**, 1543–1558.
14 Y. J. Liu, H. Y. Du, L. W. Liu and J. S. Leng, *Smart Mater. Struct.*, 2014, **23**, 023001.
15 C. Wischke, M. Behl and A. Lendlein, *Expert Opin. Drug Delivery*, 2013, **10**, 1193–1205.
16 M. C. S. L. Carbajal and G. A. Ameer, *Adv. Mater.*, 2011, **23**, 2211.
17 J. H. Yu, H. Xia and Q. Q. Ni, *J. Mater. Sci.*, 2018, **53**, 4734–4744.
18 A. Luraghi, F. Peri and L. Moroni, *J. Controlled Release*, 2021, **334**, 463–484.
19 J. Hu, M. P. Prabhakaran, L. L. Tian, X. Ding and S. Ramakrishna, *RSC Adv.*, 2015, **5**, 100256–100267.
20 J. Wu, S. Xu, C. C. Han and G. C. Yuan, *J. Controlled Release*, 2021, **321**, 472–479.
21 Y. Wang and L. Xu, *Polymers*, 2018, **10**, 144.
22 J. Wu, Z. Zhang, J. Gu, W. Zhou, X. Liang, G. Zhou, C. C. Han, S. Xu and Y. Liu, *J. Controlled Release*, 2020, **320**, 337–346.
23 H. Lian and Z. X. Meng, *Bioact. Mater.*, 2017, **2**, 96–100.
24 M. M. Chen, Y. Y. Liu, G. H. Su, F. F. Song, Y. Liu and Q. Q. Zhang, *Int. J. Nanomed.*, 2017, **12**, 4225–4239.
25 D. Kang, X. Pan, Y. Song, Y. Liu, D. Wang, X. Zhu, J. Wang and L. Hu, *Eur. J. Med. Chem.*, 2022, **243**, 114694.
26 H. Cheng, H. Zhang, G. Xu, J. Peng, Z. Wang, B. Sun, D. Aouameur, Z. Fan, W. Jiang, J. Zhou and Y. A. Ding, *Nano-Micro Lett.*, 2020, **12**, 155.
27 J. X. Zhao, Q. C. Yang, T. Wang, L. Wang, J. C. You and Y. J. Li, *ACS Appl. Mater. Interfaces*, 2017, **9**, 43415–43419.
28 C. Liu, H. Qin and P. T. Mater, *J. Mater. Chem.*, 2007, **17**, 1543–1558.
29 T. Dayyoub, A. V. Maksimkin, O. V. Filippova, V. V. Tcherdyntsev and D. V. Telyshev, *Polymers*, 2022, **14**, 3511.
30 V. Salaris, A. Leonés, D. Lopez, J. M. Kenny and L. Peponi, *Polymers*, 2022, **14**, 995.
31 A. Luraghi, F. Peri and L. Moroni, *J. Controlled Release*, 2021, **334**, 463–484.
32 G. Marosi, *eXPRESS Polym. Lett.*, 2010, **4**, 263.
33 J. X. Zhao, W. Wang, C. C. Ye, Y. J. Li and J. C. You, *J. Membr. Sci.*, 2018, **563**, 762–767.
34 C. C. Ye, J. X. Zhao, L. J. Ye, Z. Y. Jiang, J. C. You and Y. J. Li, *Polymer*, 2018, **142**, 48–51.